Microsyst Technol (2006) 12: 441–449
DOI 10.1007/s00542-005-0040-8

TECHNICAL PAPER

K. Schjølberg-Henriksen · E. Poppe · S. Moe
P. Storås · M.M.V. Taklo · D.T. Wang · H. Jakobsen

Anodic bonding of glass to aluminium

Received: 1 December 2004 / Accepted: 2 March 2005 / Published online: 21 September 2005

Abstract Anodic bonding of glass to aluminium may provide a higher degree of freedom in device design. In this paper, a systematic variation of the bonding parameters for the aluminium–glass bond is presented. Hermetic seals with strengths of 18.0 MPa can be achieved using a 50–100-nm-thick bonding aluminium layer, and bonding at 300–400°C applying a voltage of 1,000–1,500 V for 20 min. With these parameters, bond yields above 95.1% were obtained on 17 wafers. The bonds survived extensive thermal ageing without significant degradation. The possibility of bonding glass to an aluminium layer with buried, electrically isolated conductors underneath is also demonstrated.

1 Introduction

Anodic bonding is a method for sealing an alkali-rich glass to virtually any metal. The process was first described by Wallis and Pomerantz (1969) and is today a cost-effective method for wafer-level packaging. Anodic bonding gives excellent hermetic seals, and is widely used in the formation of micro-mechanical structures like pressure sensors (Hanneborg and Øhlckers 1990), accelerometers (Lapadatu et al. 2001), and microfluidic devices (Acero et al. 1997). Bonding of glass to silicon has been extensively investigated (Rogers and Kowal 1995). However, the possibility of bonding glass to materials other than silicon may provide a higher degree of freedom in the device design, and can even be essential for the realization of some devices. Therefore, anodic bonding to polysilicon (von Arx et al. 1995), thermal SiO_2 (Plaza et al. 1998), and Si_3N_4 (Weichel et al. 2000) have been subject to substantial interest.

Bonding of glass to aluminium has often been used in studies of the electrode phenomena during anodic bonding (Nitzsche et al. 1998; Arata et al. 1984). Aluminium has also been used as bonding layer for micromechanical devices (Nese and Hanneborg 1993; Veenstra et al. 2001). In this paper, a systematic variation of aluminium layer thickness and bonding parameters is presented for the first time. The hermeticity and strength of the bonds are presented. For many devices, an electrical connection between a hermetically sealed cavity and the outside world is necessary. Therefore, the possibility of forming buried aluminium feed-throughs underneath a flat bonding aluminium layer was also investigated.

2 Experimental

2.1 Anodic bonding to aluminium

2.1.1 Initial tests

For initial investigation of the bonding process, 14 pcs. 4′ silicon wafers with resistivity 2–20 Ωcm were numbered A1–A14. The wafers were thermally oxidised to a nominal oxide thickness of 650 nm. On top of the thermal oxide, an aluminium layer of thickness 50, 100, 200, or 1,200 nm was sputter deposited. Before the deposition, the thermal oxide was removed in a 5 mm wide area along the wafer edge. The aluminium was deposited on the whole wafer surface, providing elec-

K. Schjølberg-Henriksen (✉) · E. Poppe · S. Moe
P. Storås · M.M.V. Taklo · D.T. Wang
Department of Microsystems, SINTEF ICT, Blindern, 124, 0314 Oslo, Norway
E-mail: kshe@sintef.no
Tel.: +47-22-67732
Fax: +47-22-67321

H. Jakobsen
SensoNor AS, 196, 3192 Horten, Norway

Present address: H. Jakobsen
Vestfold University College, 2243, 3103 Tønsberg, Norway

trical contact between the aluminium and the bulk silicon. The wafers A1–A14 were bonded to Pyrex #7740 (Corning) glass wafers. An overview of the test wafers and the respective bonding parameters is shown in Table 1, 2.

2.1.2 Bond strength

The strength of the bonds was investigated using designated pull test structures. Three silicon wafers, numbered B1–B3, were etched in KOH to form 20 μm high frame structures. The frames were 200 μm wide, with an outer edge of 2.7 mm and an inner edge of 2.3 mm. The bonded area of each structure was hence 2 mm^2. After etching, the wafers were thermally oxidised to a nominal oxide thickness of 650 nm, and a 50-nm-thick aluminium layer was sputter deposited on top of the oxide. Before the deposition, the thermal oxide was removed in a 5 mm wide area along the wafer edge. The aluminium was deposited on the whole wafer surface, providing electrical contact between the aluminium and the bulk silicon. The wafers B1–B3 were bonded to unstructured Pyrex #7740 (Corning) glass wafers. The bonding parameters are listed in Table 1.

2.1.3 Hermeticity

The hermeticity of the bonds was tested using 17 pcs. 4′ pre-fabricated piezoresistive pressure sensor wafers from SensoNor(Knudsrødveien 7, P.O. Box 196, N-3192 Horten, Norway), numbered C1–C17. A schematic cross-section of the sensor is shown in Fig. 1. A bonding aluminium layer was sputter deposited on top of a 100-nm-thick thermal oxide. The bonding aluminium was patterned to form frames 228 μm wide at the side of the wire bond pads and 278 μm wide on the other three sides. Contact holes had previously been etched in the oxide to allow electrical contact between the bulk silicon and the bonding aluminium. The pressure sensor wafers were bonded to Pyrex #7740 (Corning) glass wafers with vacuum reference cavities. The bonding parameters are listed in Table 1.

2.1.4 Bonding

The anodic bonding was performed using an SB6 substrate bonder (SUSS MicroTec). A 3′ silicon wafer was used as plate electrode to ensure a homogeneous potential at the glass surface. To minimise oxidation of the bonding aluminium prior to bonding, the bond chamber was only heated after it had been evacuated. The bonding time was 10, 20, or 30 min. The bonding temperature was 300, 350, or 400°C, and the bonding voltage was varied between 1,000 and 2,000 V. A switch in the SB6 limited the bond current to 3 mA to protect the circuitry of the machine. An overview of the test wafers used for investigating the bonding process and their respective bonding parameters is listed in Table 1.

Table 1 Overview of the wafers used for investigating the bonding process between glass and aluminium

Type	Wafer ID	Al thickness (nm)	Bond parameters
Initial test	A1–A5	50	400°C, 1,000 V, 30 min
Initial test	A6	50	300°C, 1,000 V, 30 min
Initial test	A7	50	300°C, 1,500 V, 30 min
Initial test	A8–A9	100	400°C, 1,000 V, 30 min
Initial Test	A10–A11	200	400°C, 1,000 V, 10 min
Initial Test	A12	200	400°C, 2,000 V, 10 min
Initial Test	A13–A14	1,200	400°C, 1,000 V, 10 min
Bond strength	B1	50	400°C, 1,000 V, 30 min
Bond strength	B2	50	400°C, 2,000 V, 30 min
Bond strength	B3	50	300°C, 1,000 V, 30 min
Hermeticity	C1	50	350°C, 1,000 V, 30 min
Hermeticity	C2	50	350°C, 1,250 V, 30 min
Hermeticity	C3	50	350°C, 1,500 V, 20 min
Hermeticity	C4	50	400°C, 1,000 V, 20 min
Hermeticity	C5	50	400°C, 1,250 V, 20 min
Hermeticity	C6	50	400°C, 1,500 V, 20 min
Hermeticity	C7	100	350°C, 1,000 V, 20 min
Hermeticity	C8	100	350°C, 1,250 V, 20 min
Hermeticity	C9	100	400°C, 1,000 V, 20 min
Hermeticity	C10	100	400°C, 1,250 V, 20 min
Hermeticity	C11	100	400°C, 1,500 V, 20 min
Hermeticity	C12	200	350°C, 1,000 V, 20 min
Hermeticity	C13	200	350°C, 1,250 V, 20 min
Hermeticity	C14	200	350°C, 1,500 V, 20 min
Hermeticity	C15	200	400°C, 1,000 V, 20 min
Hermeticity	C16	200	400°C, 1,250 V, 20 min
Hermeticity	C17	200	400°C, 1,500 V, 20 min
Buried conductors	D1–D6	100	350°C, 1,000 V, until 15% of max current

Table 2 Average pull strengths, standard error and total charge for the samples from wafers B1–B3

Wafer ID	No. of samples	Bond strength (MPa)	Total charge (C)
B1	13	14.2 ± 7.3	0.77
B2	12	12.2 ± 6.0	1.62
B3	10	18.0 ± 6.4	0.57

2.1.5 *Measurement methods*

The initial test wafers A1–A14 were rated as having a "good" or "bad" bond quality. The bond quality was determined by blade tests (Maszara et al. 1988) and by visual inspection in a microscope. The bond strength wafers B1–B3 were diced into individual chips with one frame structure each. The chips were glued to grinded hexagonal head cap screws with a thin layer of Scotch 36003C glue (3 M) and pulled apart at 0.6 mm min^{-1} using the automated pull test set-up Minimat 2000 (Rheometric Scientific Inc). The glued chips are illustrated in Fig. 2, with arrows pointing at the bonded and glued interfaces. The bond strength was calculated by dividing the maximum pull force before fracture by the bonded area.

The hermeticity of the pressure sensor wafers C1–C17 was found by measuring the Wheatstone bridge output signal of each pressure sensor under atmospheric pressure using an S400 Keithley parametric test system with a TSK APM90A automatic wafer prober. Sensors with leaking cavities were recognised as having a bridge voltage signal below 16.5 mV. Sensors with bridge voltages between 16.5 and 127.5 mV were characterized as hermetically sealed. After the first hermeticity testing, wafers C7 and C9 were subjected to thermal ageing. The procedure consisted of a 240 h bake test at 150°C, 100 temperature cycles from −40 to 125°C, 240 h of exposure to 85°C and 85% relative humidity, and a helium leak test. The pressure sensors of the thermally aged wafers were then re-measured.

2.2 Buried conductor structures

The feasibility of forming buried metal structures underneath a flat bonding aluminium layer was investigated in a separate experiment. A 500-nm-thick thermal oxide was grown on six 4′ silicon wafers with resistivity 2–20 Ω cm. The wafers were numbered D1–D6. A 0.5-μm-thick aluminium layer was sputter deposited and patterned to form conductor lines. A 1.5-μm-thick plasma-enhanced chemical vapour deposition (PECVD) silicon oxide layer was deposited on top of the patterned aluminium (Dr. Philippe Langlet, Ecole Polytechnique Fédérale de Lausanne (EPFL), CH-1015, Lausanne, Switzerland) and planarised by chemical mechanical polishing (CMP) (Dr. Gerfried Zwicker, Fraunhofer Institute for Silicon Technology ISIT, Fraunhoferstraße 1, 25524 Itzehoe, Germany). A 100-nm-thick bonding aluminium layer was sputter deposited on the planarised oxide. Before the deposition, the thermal oxide was removed in a 5 mm wide area along the wafer edge. The aluminium was deposited on the whole wafer surface, providing electrical contact between the aluminium and the bulk silicon. The wafers were bonded to unstructured Pyrex #7740 (Corning) glass wafers at 350°C applying a bias of 1,250 V. The bonding bias was applied until the bonding current had decayed to 15% of its maximum value. The bonding parameters are listed in Table 1. The cross-section of the bonded wafers is illustrated in Fig. 3.

Before deposition of the bonding aluminium layer, the roughness of the polished PECVD oxide surface was measured by atomic force microscopy (AFM) in contact mode and tapping mode. A Nanoscope (Digital Instruments) was used. A sample was cut from each of the wafers D2 and D5. One area far away from the buried aluminium lines and one area on top of the lines were imaged on each sample. After deposition of the bonding aluminium, the planarity of the polished wafers was investigated by WYKO white light interferometry (Veeco). All six wafers were measured in at least three different locations: at the centre of the wafer, midway between centre and the wafer edge, and close to the wafer edge.

After bonding, all wafer pairs were inspected visually. One bonded wafer stack (D4) was diced to make cross-section samples. The cross-section of the bonded interface was studied with a Philips CM30 transmission electron microscope (TEM).

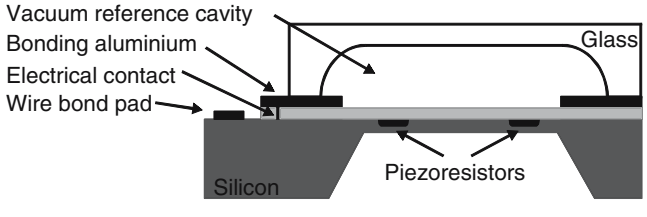

Fig. 1 Schematic cross-section of the pressure sensor used for hermeticity tests of the bonds

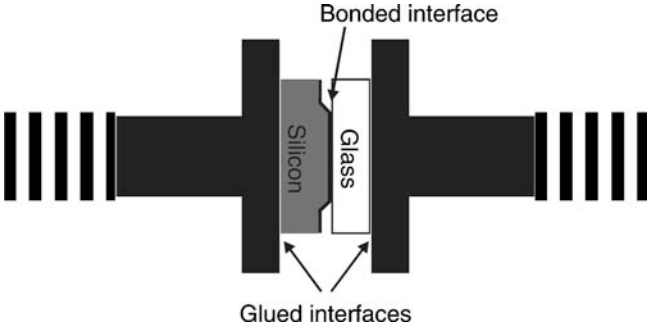

Fig. 2 Chips for bond strength measurement glued to screws for pull testing

3 Results

3.1 Initial tests and hermeticity

The wafers A13–A14, with 1.2-μm-thick bonding aluminium, delaminated easily during the blade test, and were characterised as having a "bad" bond quality. After delamination, the glass had a dotted appearance with a pattern corresponding to typical sintering hillocks. Wafers A1–A12, with a bonding aluminium of 200 nm or thinner, crushed into very small pieces as the blade was forced between the bonded wafers. It was evident that the bonds were strong. All wafers A1–D6 appeared to bond well. A plot of the parameters during a typical bonding process is shown in Fig. 4. After bonding, the bonding aluminium of thickness 200 nm or less had a speckled appearance. The speckles showed as black spots with diameter 2–20 μm. Figure 5 shows the corner of a pressure sensor die with speckled aluminium.

Figure 6 shows the yield for the pressure sensor wafers C1–C17, grouped by bond metal thickness, bonding voltage, and bonding temperature. For the two latter categories, the yield is plotted only for samples with 50- and 100-nm-thick bonding aluminium, since the yield for 200-nm-thick aluminium was so much lower. The typical bridge signal of a good die after bonding was 54 mV. After the thermal ageing, 40 randomly selected dies from wafers C7 and C9 were re-measured manually. These thermally aged dies had an average bridge voltage signal of 34 mV.

3.2 Bond strength

The bond strengths of the samples from wafers B1–B3 are listed in Table 2. The average and standard deviation of the sample sets are listed. The fracture probabilities were illustrated by Weibull plots (Weibull 1939), and are plotted in Fig. 7. The total charge involved in the bonding process was calculated by integrating the bonding current over bonding time.

3.3 Buried conductor structures

The AFM measurements indicated that the polished PECVD oxide surface was flat. The surface level was not significantly higher on top of the buried aluminium lines. The surface roughness was below 0.7 nm for areas 10×10 μm^2. However, images taken in areas both with and without a buried aluminium line showed trenches in the oxide at the position of the buried aluminium line. The trenches were up to 200 nm wide and ran along the edges of the buried aluminium lines. The distance between the trenches was measured to be 21 ± 0.5 μm for a nominally 20 μm wide aluminium line.

The WYKO images were taken after deposition of the bonding aluminium, but before bonding. The buried

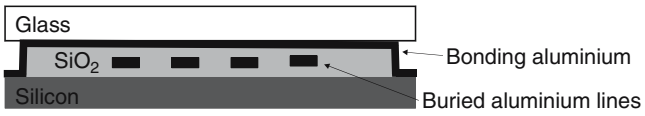

Fig. 3 Cross-section of the bonded test wafers

aluminium lines were clearly visible on all wafers D1–D6. A sample image from the edge of wafer D6 is shown in Fig. 8. An area of 600×450 μm^2 was measured. The rms-values for the surface roughness were between 3.7 and 4.5 nm for all six wafers. The maximum height difference on the surface was 11–12 nm, but most lines were only slightly higher than the rms-roughness of the surface.

After bonding, wafers D1–D6 were inspected visually in a microscope. The pattern of the buried aluminium lines could be observed through the bonded glass. The pattern was caused by differences in the speckles of the bonding aluminium. This is illustrated in Fig. 9. In the areas without buried aluminium underneath, the bonding aluminium was speckled similarly to the wafers A–C as seen in Fig. 5. The speckles appeared as black spots with diameter 2–4 μm. In the areas with buried aluminium lines, there were fewer speckles.

The cross-section of the bonded interface of wafer D4 was studied by TEM. Figure 10 shows a cross-section of the bonded interface. Sections both with and without a buried aluminium line are shown. Two cracks, seen as bright lines, are visible in the picture. One runs from the corner of the buried aluminium line to the bonding aluminium. The other crack runs between the glass and the bonding aluminium to the left in Fig. 10. The silicon and oxide materials in Fig. 10 show fairly uniform contrast. In the glass, we see the depletion line, parallel to the bonding interface, approximately 1.5 μm into the glass.

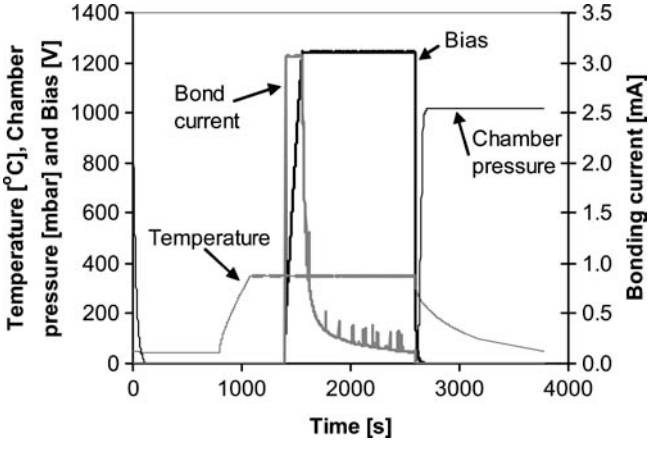

Fig. 4 Plot of bonding parameters versus time for a typical bonding process. The temperature, chamber pressure, and bonding bias are shown on the axis to the left, while the bonding current is shown on the axis to the right. The bonded wafer is C2

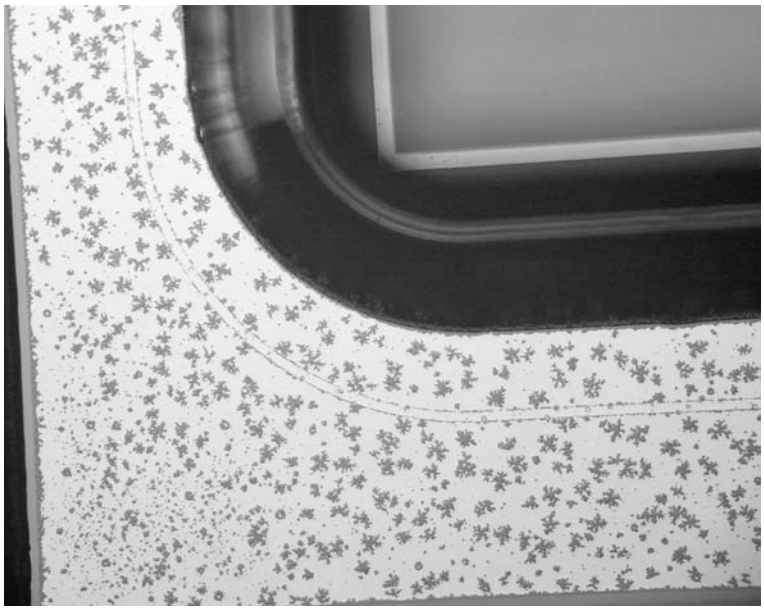

Fig. 5 Corner of a pressure sensor die after bonding. speckles with diameter 2–20 μm were seen in the bonding aluminium

Figure 10 also shows dark lines, about 0.1–0.2 μm long, extending from the bonding aluminium into the glass. These dark lines were present in both areas with and without buried aluminium lines. The analysis of the dark lines showed that they contained aluminium. In addition, there were bright dendrites running from the buried aluminium lines to the bonding aluminium. The material of these dendrites could not be identified, but it was non-crystalline and less dense than SiO_2, since it appeared brighter than SiO_2 in the TEM image. A higher magnification image of the dendrites is shown in Fig. 11.

The TEM analysis revealed some voids in the bonding aluminium. These can be seen as bright areas in Fig. 12. The diameters of the two measured voids were 0.3 and 0.4 μm.

4 Discussion

The poor bond quality of the wafers with 1.2-μm-thick bonding aluminium and the results from Fig. 6 clearly indicate that the bond quality increased with decreasing thickness of the bonding aluminium. This was probably due to the large mismatch in thermal coefficient of expansion (TCE) between aluminium and silicon. During bonding at 300–400°C, aluminium (TCE = 23.1 ppm K^{-1}) expanded more than silicon (TCE = 2.6 ppm K^{-1}), and upon cooling, a thermally induced stress was created. Other workers (Arata et al. 1984; van Helvoort et al. 2003; van Helvoort and Knowles 2003) have reported thermal stress to cause 1-

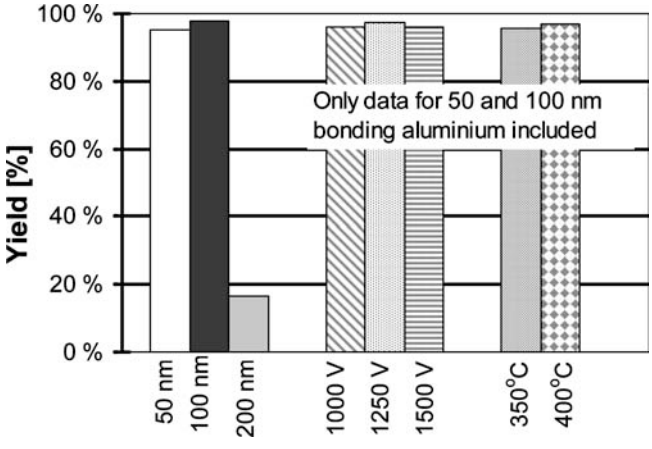

Fig. 6 Bond yield grouped by bonding aluminium thickness, bonding voltage, and bonding temperature for wafers C1–C17. For the two latter categories, only samples with 50 and 100 nm metal were included

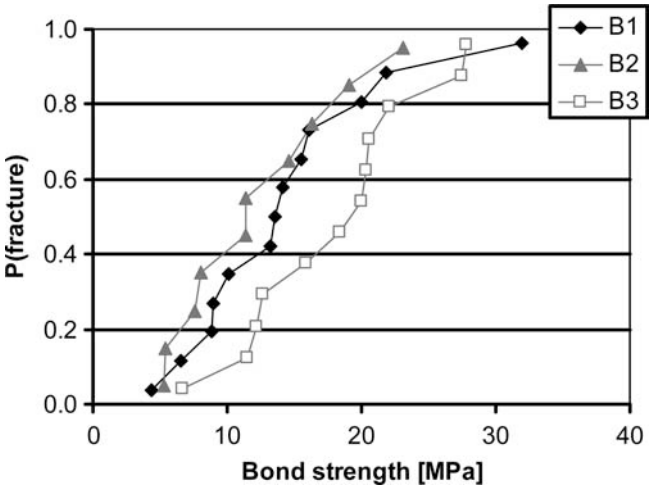

Fig. 7 The Weibull plot shows the probability for fracture at a given applied pressure. Grey lines denote 1,000 V bonding bias, black lines denote 2,000 V bonding bias. Open symbols represent 300°C bonding temperature, and filled symbols represent for 400°C

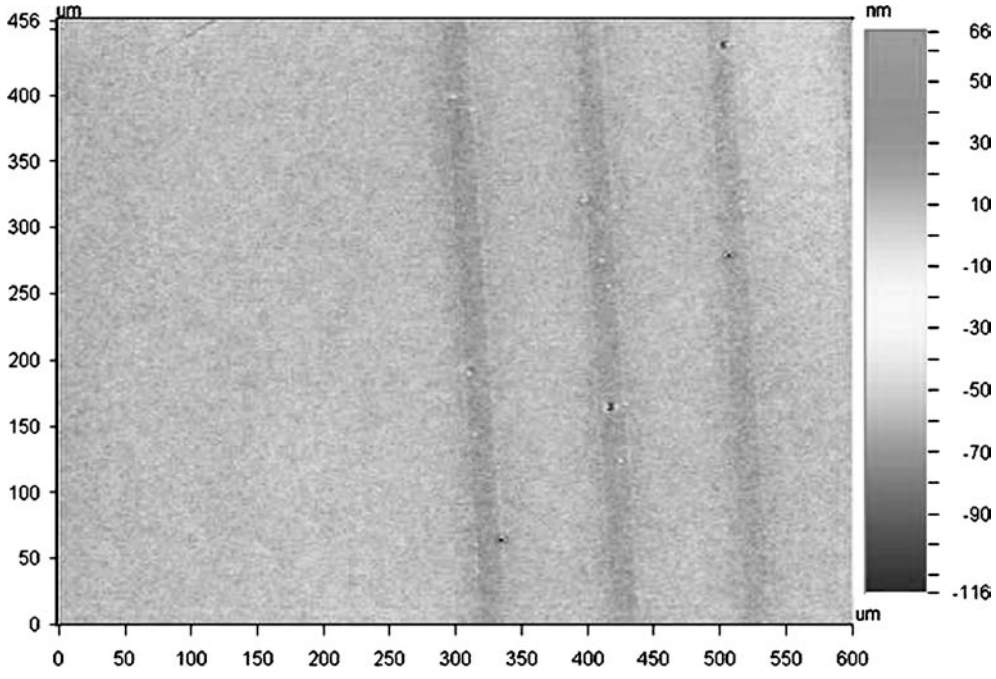

Fig. 8 WYKO image from the edge of wafer D6. Aluminium has been deposited on top of the polished SiO_2. The lines buried within the SiO_2 are clearly visible as a higher surface level on the wafer

and 3-mm-thick glass to break in the bulk when bonded to 0.5- and 2-mm-thick aluminium pieces.

In our case, the thin films probably allowed for a restructuring of the aluminium through the formation of small hillocks, and sufficiently low stress resulted for 50- and 100-nm-thick bonding aluminium. Hence the high yields of 95.1 and 97.7%, as seen in Fig. 6, were obtained. The stress created in 200-nm-thick bonding aluminium significantly deteriorated the bond quality and reduced the yield to 16.7%. The 1.2-μm-thick bonding aluminium caused too high stresses for the bond to withstand even careful mechanical handling.

Figure 6 further shows that for bonding aluminium thicknesses of 50 and 100 nm, all the combinations of bonding temperature and bonding bias gave yields above 95.1%. This implies that bonding at temperatures between 350 and 400°C applying biases between 1,000 and 1,500 V can be expected to give good results. The bonding time of 20 min was sufficient to create these high yields meaning that bonding to aluminium is well suited as an industrial process where short process times are crucial.

Figure 5 shows an example of the speckled appearance of the bonding aluminium after bonding. Speckles were observed on all wafers with a bonding aluminium of 200 nm or thinner. The characteristics of the speckles have not yet been identified. The image in Fig. 5 shows that the typical speckle diameter was 2–20 μm. The TEM pictures in Fig. 12 shows that the diameter of the

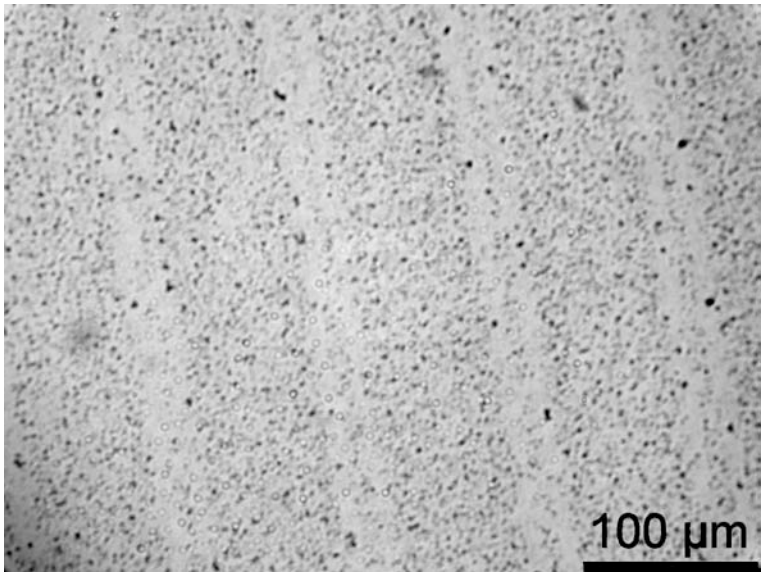

Fig. 9 Wafer D3 after bonding. The surface of the bonding aluminium had a speckled appearance on top of the SiO_2 where there was no buried Al line. The bonding aluminium on SiO_2 on top of buried Al lines, did not have similar speckles

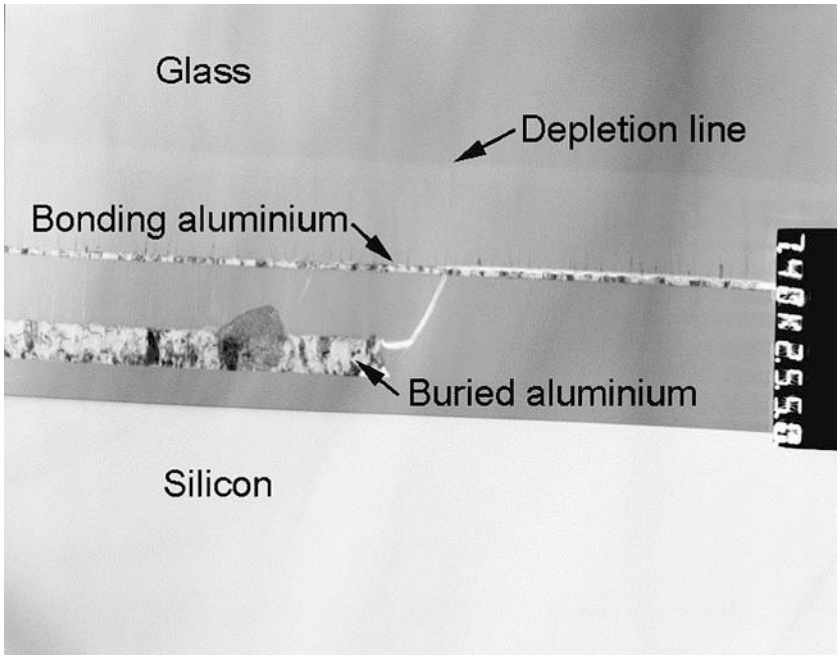

Fig. 10 Cross-section of the bonded interface of wafer D4. The cross-section shows the glass, the bonding aluminium, and the silicon. On the right side of the picture, there is a buried aluminium line, whereas to the left, there is no buried aluminium line

micro voids was 0.3–0.4 μm. Hence, it is very unlikely that the speckles were voids. Neither did the TEM analysis show any areas with a different material composition or other deviations that could explain the nature of the speckle. Rather, two observations suggest that the speckles were related to the mechanical mechanism of the bonding. Speckles were not observed on wafers A13–A14, which had 1.2-nm-thick bonding aluminium, and bonded poorly. The thick bonding aluminium probably had a less smooth surface and several hillocks, preventing large areas of intimate contact between the wafers to be bonded. This could explain the poor bond and the lack of speckles on wafers A13 and A14. In addition, on wafers D1–D6, we observed that the areas with and without buried aluminium lines were speckled differently. This suggests that the speckles could be the points where the first onset of bonding occurred, or areas where several bonding fronts met and formed a somewhat different bond.

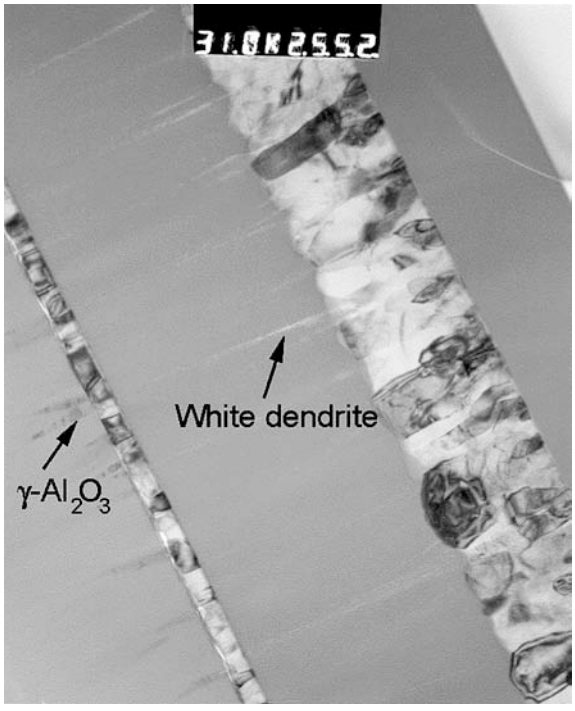

Fig. 11 Cross-section of the bonded interface at the area of a buried aluminium line. The two arrows point at a dark line of γ-aluminium oxide extending into the glass and at the bright dendrite running from the buried aluminium towards the bonding aluminium

Figure 6 shows that even with a speckled bonding aluminium, more than 95% of the pressure sensors were hermetically sealed. This observation also supports the conclusion that the speckles were not voids. The micro voids shown in Fig. 12 are not expected to affect the hermeticity, unless a network of the voids can be formed. The hermeticity of sensors with buried conductors, as shown in Fig. 3, must be further investigated. Figure 10 shows a crack running from the buried aluminium to the bonding aluminium along the length of the buried aluminium line. The cracking could be caused by tensile stress in the PECVD oxide, and could possibly be controlled by adequate doping of the deposited oxide (Plummer et al. 2000). This issue must be further investigated.

The results in Fig. 7 and show that high bond strengths can be achieved. Bonding glass to a 50-nm-thick aluminium layer applying 1,000 V at 300°C gave an average bond strength of 18.0 ± 6.4 MPa. This is comparable to the strength of glass–silicon bonds of 10–15 and up to 30 MPa reported in the literature (Lee

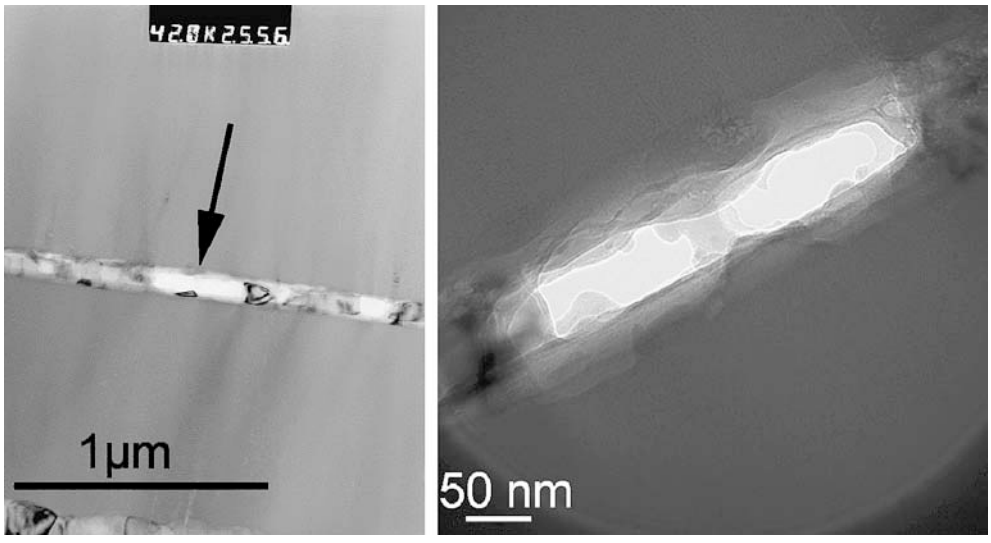

Fig. 12 Voids in the bonding aluminium. To the left, the diameter of the void is around 0.4 µm. To the right, the measurement bar in the picture is 50 nm, and the void diameter is around 0.3 µm

et al. 2000; Obermeier 1995). The bond strengths of 12–18 MPa obtained in this work are higher than the 6–10 MPa reported for anodic bonding to thin-film deposited glass (Visser et al. 2002a), the 10 MPa reported for gold thermo compression bonding (Taklo et al. 2004), and the 4–8 MPa reported for plasma activated bonding (Visser et al. 2002b). The TEM pictures in Fig. 11 shows γ-Al_2O_3 dendrites extending from the bonding aluminium and into the glass. Van Helvoort et al. (van Helvoort et al. 2003; van Helvoort and Knowles 2003) have argued the presence of such dendrites to be an indicator of a strong bond.

The thermal ageing procedure described in subsection "Measurement Methods" typically decreased the bridge voltage signal by 20 mV. All the 40 dies that were re-measured still had bridge voltages within the specifications after the thermal ageing. The bridge voltage decrease could be caused by changes in contact resistance of the pads, temperature cycling effects of the aluminium, or other electrical properties of the pressure sensors. However, slightly leaking seals cannot be out ruled. Helium has been shown to be able to diffuse through glass (Altemose 1961). It is possible that helium gas diffused through the bulk glass during the helium leak test, increasing the pressure in the reference cavity. To verify the hermeticity of thermally aged dies, further long-term testing must be performed.

5 Conclusion

A systematic variation of the bonding parameters for the aluminium–glass bond has been presented. Hermetic seals with yields above 95% and strengths as high as 18.0 MPa can be achieved using a 50–100-nm-thick bonding aluminium layer, and bonding at 300–400°C applying a voltage of 1,000–1,500 V for 20 min. The bonds survived extensive thermal ageing without significant degradation. This work proves the suitability of the glass–aluminium bond as an industrial process. The possibility of bonding glass to an aluminium layer with buried, electrically isolated conductors underneath, has also been demonstrated.

References

Acero MC, Plaza JA, Esteve J, Carmona M, Marco S, Samitier J (1997) Design of a modular micropump based on anodic bonding. J Micromech Microeng 7:179–182

Altemose VO (1961) Helium diffusion through glass. J Appl Phys 32:1309–1316

Arata Y, Ohmori A, Sang S, Okamoto I (1984) Pressure and field-assisted bonding of glass to aluminium. Trans JWRI 13:35–40

Hanneborg A, Øhlckers P (1990) A capacitive silicon pressure sensor with low TC_0 and high long-term stability. Sens Act A21–23:151–154

Lapadatu D, Habibi S, Reppen B, Salomonsen G, Kvisterøy T (2001) Dual-axes capacitive inclinometer/low-g accelerometer for automotive applications. Tech. Digest 14th IEEE Intl Conf MEMS, Interlaken, Switzerland, 34–37

Lee TMH, Lee DHY, Liaw CYN, Lao AIK, Hsing IM (2000) Detailed characterization of anodic bonding process between glass and thin-film coated silicon substrates. Sens Act A 86:103–107

Maszara WP, Goetz G, Caviglia A, McKitterick JB (1988) Bonding of silicon wafers for silicon-on-insulator. J Appl Phys 64:4943–4950

Nese M, Hanneborg A (1993) Anodic bonding of silicon to silicon wafers coated with aluminium, silicon oxide, polysilicon or silicon nitride. Sens Act A 37(38):61–67

Nitzsche P, Lange K, Schmidt B, Grigull S, Kreissig U, Thomas B, Herzog K (1998) Ion drift processes in Pyrex–Typr alkali–borosilicate glass during anodic bonding. J Electrochem Soc 145:1755–1762

Obermeier E (1995) Anodic wafer bonding. In: Hunt CE, Baumgart H, Iyer SS, Abe T, Gösele U (eds) Semiconductor wafer bonding: science, technology, and applications III. The Electrochemical Society, Pennington, NJ, pp 212–220

Plaza JA, Esteve J, Lora-Tamayo E (1998) Effect of silicon oxide, silicon nitrode and polysilicon layers on the electrostatic pressure during anodic bonding. Sens Act A 67:181–184

Plummer JD, Deal MD, Griffin PB (2000) Silicon VLSI Technology, fundamentals, practice and modelling. Prentice Hall, Upper Saddle River, New Jersey

Rogers T, Kowal J (1995) Selection of glass, anodic bonding conditions and material compatibility for silicon–glass capacitive sensors. Sens Act A 46–47:113–120

Taklo MMV, Storås P, Schjølberg-Henriksen K, Kasting HK, Jakobsen H (2004) Strong, high-yield and low-temperature thermocompression silicon wafer-level bonding with gold. J Micromech Microeng 14:884–890

van Helvoort ATJ, Knowles KM (2003) Nanostructures at electrostatic bond interfaces. J Am Ceram Soc 86:1773–1776

van Helvoort ATJ, Knowles KM, Fernie JA (2003) Interfacial microstructures of silicon–Pyrex electrostatic bonds. J Cer Proc Res 4:1–8

Veenstra TT, Berenschot JW, Gardeniers JGE, Sanders RGP, Elwenspoek MC, van den Berg A (2001) Use of selective anodic bonding to create micropump chambers with virtually no dead volume. J Electrochem Soc 148:G68–G72

Visser MM, Wang DT, Hanneborg AB (2002a) Fast silicon to silicon wafer bonding with an intermediate glass film. In: Baumgart H, Hunt CE, Bengtsson S, Abe T (eds) Semiconductor wafer bonding: science, technology, and applications VI. The Electrochemical Society, Pennington, NJ, pp 74–83

Visser MM, Weichel S, deReus R, Hanneborg A (2002b) Strength and leak testing of plasma activated bonded interfaces. Sens Act A97–98:434–440

von Arx J, Ziaie B, Dokmeci M, Najafi K (1995) Hermeticity testing of glass–silicon packages with on-chip feedthroughs. Tech Digest 8th Transducers, Stockholm, Sweden, 244–247

Wallis G, Pomerantz DI (1969) Field-assisted glass–metal sealing. J Appl Phys 40:3946–3949

Weibull W (1939) Statistical theory of the strength of materials. Ingenjörsvetenskapsakademins Handlingar 151:1–45

Weichel S, deReus R, Bouaidat S, Rasmussen PA, Hansen O, Birkelund K, Dirac H (2000) Low-temperature anodic bonding to silicon nitride. Sens Act A 82:249–253